Basic Research

OPEN

Staphylococcus aureus From an Acute Fracture-related Infection Displays Important Bacteriological and Histopathologic Differences From a Chronic Equivalent in a Murine Bone Infection Model

Susanne Baertl MD[1,2], Lena Gens DVM[2], Dirk Nehrbass DVM[2], Eric T. Sumrall PhD[2,3],
Stephan Zeiter DVM, PhD[2] , Gopala Krishna Mannala PhD[1], Markus Rupp MD[1], Nike Walter PhD[1],
R. Geoff Richards Prof[2], T. Fintan Moriarty PhD[2], Volker Alt Prof[1]

Abstract

Background *Staphylococcus aureus* is the leading pathogen in fracture-related infection. Previous in vitro experiments, in vivo testing in wax moth larvae, and genomic analysis of clinical *S. aureu*s isolates from fracture-related infection identified low-virulence (Lo-SA5464) and high-virulence (Hi-SA5458) strains. These

findings correlated with acute fracture-related infection induced by Hi-SA5458, whereas Lo-SA5464 caused a chronic fracture-related infection in its human host. However, it remains unclear whether and to what extent the causative pathogen is attributable to these disparities in fracture-related infections.

Question/purpose Are there differences in the course of infection when comparing these two different clinical isolates in a murine fracture-related infection model, as measured by (1) clinical observations of weight loss, (2) quantitative bacteriology, (3) immune response, and (4) radiographic and histopathologic morphology?

Methods Twenty-five (including one replacement animal) female (no sex-specific influences expected), skeletally mature C57Bl/6N inbred mice between 20 and 28 weeks old underwent femoral osteotomy stabilized by titanium locking plates. Fracture-related infection was established by inoculation of high-virulence *S. aureus* EDCC 5458 (Hi-SA5458) or low-virulence *S. aureus* EDCC 5464 (Lo-SA5464) in the fracture gap. Each of these groups consisted of 12 randomly assigned animals. Mice were euthanized 4 and 14 days postsurgery, resulting in six animals per group and timepoint. The severity and progression of infection were assessed in terms of clinical observation of weight loss, quantitative bacteriology, quantitative serum cytokine levels, qualitative analysis of postmortem radiographs, and semiquantitative histopathologic evaluation.

Results For clinical observations of weight change, no differences were seen at Day 4 between Hi-SA5458- and Lo-SA5464-infected animals (mean -0.6 ± 0.1 grams

[1]Regensburg University Medical Center, Department of Trauma Surgery, Regensburg, Germany

[2]AO Research Institute Davos, Davos-Platz, Switzerland

[3]Harvard Medical School, Department of Microbiology, Boston, MA, USA

V. Alt ✉, Regensburg University Medical Center, Department of Trauma Surgery, Regensburg, Germany, Email: Volker.alt@ukr.de

versus -0.8 ± 0.2 grams, mean difference -0.2 grams [95% CI -0.8 to 0.5 grams]; p =0.43), while at 14 days, the Hi-SA5458 group lost more weight than the Lo-SA5464 group (mean -1.55 ± 0.2 grams versus -0.8 ± 0.3 grams; mean difference 0.7 grams [95% CI 0.2 to 1.3 grams]; p = 0.02). Quantitative bacteriological results 4 days postoperatively revealed a higher bacterial load in soft tissue samples in Hi-SA5458-infected animals than in the Lo-SA5464-infected cohort (median 6.8×10^7 colony-forming units [CFU]/g, range 2.2×10^7 to 2.1×10^9 CFU/g versus median 6.0×10^6 CFU/g, range 1.8×10^5 to 1.3×10^8 CFU/g; difference of medians 6.2×10^7 CFU/g; p = 0.03). At both timepoints, mice infected with the Hi-SA5458 strain also displayed higher proportions of bacterial dissemination into organs than Lo-SA5464-infected animals (67% [24 of 36 organs] versus 14% [five of 36 organs]; OR 12.0 [95% CI 3.7 to 36]; p < 0.001). This was accompanied by a pronounced proinflammatory response on Day 14, indicated by increased serum cytokine levels of interleukin-1β (mean 9.0 ± 2.2 pg/mL versus 5.3 ± 1.5 pg/mL; mean difference 3.6 pg/mL [95% CI 2.0 to 5.2 pg/mL]; p < 0.001), IL-6 (mean 458.6 ± 370.7 pg/mL versus 201.0 ±89.6 pg/mL; mean difference 257.6 pg/mL [95% CI 68.7 to 446.5 pg/mL]; p = 0.006), IL-10 (mean 15.9 ± 3.5 pg/mL versus 9.9 ± 1.0 pg/mL; mean difference 6.0 pg/mL [95% CI 3.2 to 8.7 pg/mL]; p < 0.001), and interferon-γ (mean 2.7 ± 1.9 pg/mL versus 0.8 ± 0.3 pg/mL; mean difference 1.8 pg/mL [95% CI 0.5 to 3.1 pg/mL]; p = 0.002) in Hi-SA5458-infected compared with Lo-SA5464-infected animals. The semiquantitative histopathologic assessment on Day 4 revealed higher grades of granulocyte infiltration in Hi-SA5458-infected animals (mean grade 2.5 ± 1.0) than in Lo-SA5464-infected animals (mean grade 1.8 ± 1.4; mean difference 0.7 [95% CI 0.001 to 1.4]; p = 0.0498). On Day 14, bone healing at the fracture site was present to a higher extent in Lo-SA5464-infected animals than in Hi-SA5458-infected animals (mean grade 0.2 ± 0.4 versus 1.8 ± 1.2; mean difference -1.6 [95% CI -2.8 to -0.5]; p = 0.008).

Conclusion Similar to septic infection in a human host, infection with Hi-SA5458 in this murine model was characterized by a higher bacterial load, more-pronounced systemic dissemination, and stronger systemic and local inflammation. Thus, there is strong support for the idea that pathogenic virulence plays a crucial role in fracture-related infections. To confirm our observations, future studies should focus on characterizing *S. aureus* virulence at the genomic and transcriptomic levels in more clinical isolates and patients. Comparing knockout and wildtype strains in vitro and in vivo, including the *S. aureus* strains studied, could confirm our findings and identify the genomic features responsible for *S. aureus* virulence in fracture-related infections.

Clinical Relevance For translational use, virulence profiles of *S. aureus* may be useful in guiding treatment

decisions in the future. Once specific virulence targets are identified, one approach to fracture-related infections with high-virulence strains might be the development of anti-virulence agents, particularly to treat or prevent septic dissemination. For fracture-related infections with low virulence, prolonged antimicrobial therapy or exchange of an indwelling implant might be beneficial owing to slower growth and persistence capacity.

Introduction

Fracture-related infection is one of the most devastating complications in modern trauma surgery [16]. *Staphylococcus aureus* is the most common pathogen in fracture-related infections, accounting for more than 30% of cases [22, 26, 28]. The clinical course of *S. aureus* fracture-related infection may be acute and aggressive, or it might be a more benign but recalcitrant chronic infection. These disparities could be attributable to the surgical procedure, adequacy of antimicrobial therapy, host's immune response, or virulence of the infectious pathogen [12,16]. Trouillet-Assant et al. [27] found that *S. aureus* isolates that were retrieved during chronic and recurrent bone and joint infections resulted in reduced cytotoxicity, mortality, virulence, and host immune escape compared with their ancestral isolates in a mouse infection model, and they were associated with increased intraosteoblastic persistence and biofilm formation. Recently performed in vitro and in vivo research compared various clinical *S. aureus* strains isolated from different patients with chronic or acute fracture-related infections [14]. One patient with acute and septic infection was selected to provide a high-virulence phenotype (Hi-SA5458), and a second patient with a chronic fracture-related infection with no clinical signs of infection except for persistent pain because of delayed bone healing was selected to provide the low-virulence isolate (Lo-SA5464). In vitro testing of both strains revealed that Hi-SA5458 possessed a stronger biofilm-forming ability and increased invasion and proliferation inside osteoblast-like cells than the Lo-SA5464 strain. Additionally, Hi-SA5458 resulted in increased mortality of Galleria mellonella larvae [14]. Finally, the Lo-SA5464 isolate had mutations affecting virulence regulators including AgrC and SarU, members of the Agr and SarA protein families [14]. The Agr and SarA systems are important for the formation of bacterial abscesses and biofilms and for expressing various toxins that mediate cell lysis, bone resorption, and maintenance of a proinflammatory environment [2, 3, 19].

Several factors influencing the course of fracture-related infections have been described [16]. A time-related classification in acute and chronic fracture-related infections is still used to guide surgical and antimicrobial treatment strategies. However, there is growing controversy about

this time-related classification because it oversimplifies the complexity of fracture-related infection [1, 7, 16, 18]. Further, the host's comorbidities and immune status may impact the clinical presentation, course, and systemic dissemination of infection [1, 17]. Recently, specific virulence characteristics of *S. aureus* have been detected in clinical isolates of acute and chronic bone infections, suggesting these characteristics may play a key role in infection development and persistence [3]. These findings, most of which were obtained from osteomyelitis models in animals or in vitro assays comparing knockout strains with wild types, have provided valuable insights into bacterial virulence in bone infections [11, 13, 29]. However, although the clinical and investigative findings may be similar, results derived from osteomyelitis models cannot be automatically extrapolated to fracture-related infections [17]. In contrast to osteomyelitis, the presence of a fracture and influence of a frequently inserted implant may differentially affect the regulatory network, so the role of bacterial virulence in the pathophysiology of fracture-related infection remains unclear. Thus, detailed bacteriologic and histopathologic analyses of clinical isolates that may differ in bacterial virulence because of variations in genomic sequences and their association with the clinical and pathophysiologic course of fracture-related infections are still lacking [3, 29].

We therefore asked: Are there differences in the course of infection when comparing these two different clinical isolates in a murine fracture-related infection model, as measured by (1) clinical observations of weight loss, (2) quantitative bacteriology, (3) immune response, and (4) radiographic and histopathologic morphology?

Material and Methods

Experimental Overview

A murine bone infection model was used to comparatively evaluate the clinical course of fracture-related infection with two different *S. aureus* isolates (*S. aureus* EDCC 5458 [Hi-SA5458] versus *S. aureus* EDCC 5464 [Lo-SA5464]) in terms of local and systemic characteristics (Fig. 1). Mice received osteotomy of the left femur stabilized by a locking plate. The fracture gap was inoculated with Hi-SA5458 (n = 12) or Lo-SA5464 (n = 12). To assess the course of infection, two timepoints for euthanasia were set, 4 and 14 days postsurgery, resulting in a final group of six animals per subgroup and timepoint. Outcome parameters were quantitative assessment of weight change, quantitative bacteriology in the soft tissue and harvested organs, quantitative assessment of serum cytokine levels to measure the systemic immune response, qualitative assessment of present callus

formation on radiographs, and semiquantitative histopathologic grading by a veterinary pathologist (DN). All analyses were performed in a blinded manner, and group assignment was not announced until data collection was completed.

Bacteria

Clinical strains were obtained from two male patients treated for fracture-related infections (Table 1). The genome sequences of both strains are available in the public ENA/NCBI/DNA databases under accession numbers CP022290 (*S. aureus* EDCC 5458) and CP022291 (*S. aureus* EDCC 5464). To facilitate readability, *S. aureus* EDCC 5458, which is considered a high-virulence pathogen, is referred to as Hi-SA5458, and *S. aureus* EDCC 5464, which was presumed to be low-virulence, is referred to as Lo-SA5464.

Animals

Female inbred C57Bl/6N mice (25, including replacement mice) were purchased from Charles River Laboratories. The animals were at least 20 to 28 weeks old at the time of surgery. Mice were acclimatized to the facility and cage mates for at least 2 weeks before surgery. Mice (six animals per subgroup and timepoint) were inoculated with Hi-SA5458 or Lo-SA5464 and euthanized at Days 4 and 14 postoperatively. Animals were randomly allocated to their respective groups, with surgeons and animal caretakers blinded to group assignment. All mice were placed in their respective groups (three per cage), according to group allocation for the study and housed in individually ventilated cages (IVC; Techniplast and Allentown) with a 12-hour light-dark cycle. Food (KLIBA NAFAG number 3436, Provimi Kliba AG) and water were available ad libitum.

Inoculum Preparation

Hi-SA5458 and Lo-SA5464 were kept as frozen stocks and stored at -20°C until use. The day before surgery, an overnight culture of both strains was prepared in 5-mL tryptic soy broth (Oxoid) and placed in a shaking incubator at 37°C. On the day of surgery, a fresh subculture was prepared in tryptic soy broth and incubated for 2 hours under the same conditions. Bacteria were washed twice with phosphate-buffered saline (Gibco) and resuspended in 5 mL of phosphate-buffered saline. This bacterial suspension was sonicated in an ultrasound water bath (Bandelin Sonorex Super 10P, Bandelin) at 40 kHz
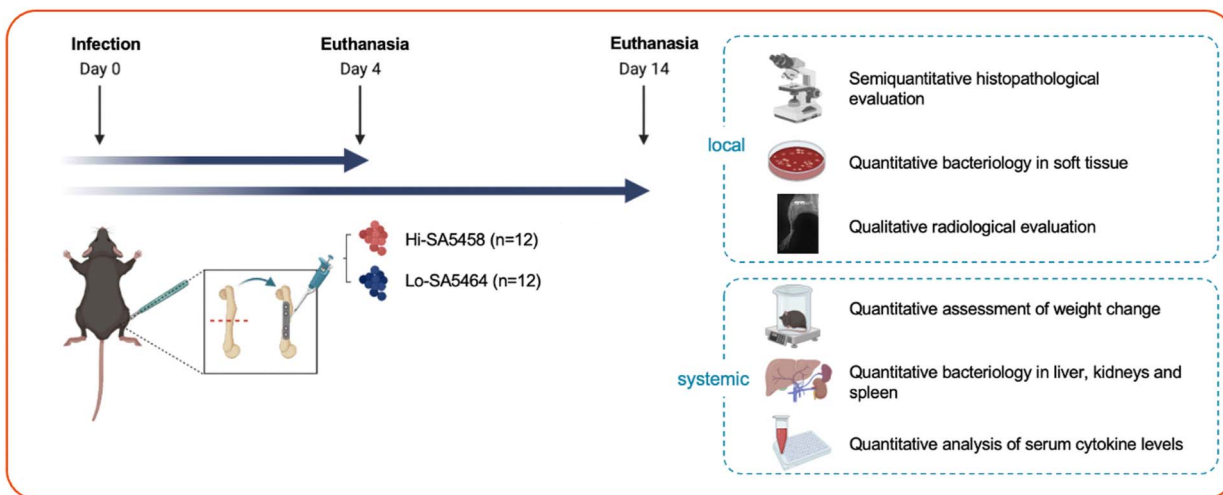
Fig. 1 This figure shows an experimental overview of the study design. In total, 24 mice were subjected to femoral osteotomy, which was stabilized by a locking plate (Day 0). Either Hi-SA5458 (n = 12) or Lo-SA5464 (n = 12) was inoculated into the fracture gap. Animals were euthanized on Days 4 and 14, resulting in six animals per subgroup (Hi-SA5458 or Lo-SA5464) and timepoint. Local infection characteristics were assessed with a semiquantitative histopathologic evaluation of the bone and soft tissue, quantitative bacteriology in the soft tissue, and qualitative evaluation of callus formation on postmortem radiographs. Systemically, a quantitative assessment of weight loss, quantitative bacteriology in harvested organs, and quantitative assessment of serum cytokine levels were performed.

for 3 minutes. The optical density of the bacterial solution was measured at 600 nm by spectrophotometry using a MultiskanTM GO spectrophotometer (ThermoFisher Scientific).

The resulting suspension was diluted to an OD600 of 0.02 for a total of approximately 1×10^4 colony-forming units (CFUs) per 1 μL. The actual number of bacteria in the suspension and in the inoculum was quantified by performing six serial 10-fold dilutions and plating of 10 μL of all dilutions on tryptic soy agar plates in technical triplicates. Plates were incubated for 24 hours at 37°C, and CFUs were counted.

Surgical Intervention and Postoperative Care

The mice were anesthetized by induction with sevoflurane (approximately 5% in O_2, flow rate 1 L/minute; Sevofluran Baxter®, Baxter AG, Opfikon) and maintained during surgery with sevoflurane (approximately 2% to 3% in O_2, flow rate 0.4 to 0.6 L/minute) through a face mask.

The left femur was stabilized by a titanium four-hole MouseFix locking plate (RISystems AG) and fixed with four self-cutting, angular stable screws (RISystems). A 0.44-mm osteotomy was subsequently performed using the MouseFix Drill-&Saw guide (RISystems) and a Gigli

Table 1. Patient characteristics with respect to the isolated strains of *S. aureus* used in this study [16]

Patient characteristic	Hi-SA5458	Lo-SA5464
Age in years	54	70
Sex	Male	Male
Anatomic site	Distal femur	Distal fibula and tibia
Implant	Plate osteosynthesis	Plate osteosynthesis (fibula) and intramedullary nail (tibia)
Type[a]	Acute fracture-related infection	Chronic fracture-related infection
CRP level (mg/mL)[b]	479	14
Clinical symptoms	Redness, swelling, purulent drainage, fever	Delayed bone healing

[a]Acute (< 6 weeks) and chronic (> 6 weeks) fracture-related infection were distinguished according to the time interval to onset of infection after fracture fixation.
[b]CRP levels at the time of admission to the hospital. CRP = C-reactive protein.

hand saw (RISystems, Gigly wire saw with 0.44-mm diameter). Afterwards, an inoculum (1 µL) was pipetted into the fracture gap. Osteotomy and implant positions were confirmed radiographically in the lateral plane immediately postoperatively. Thereafter, lateral radiographs were taken on the day of euthanasia (Days 4 and 14 postsurgery).

Postoperative analgesia was provided with tramadol (25 mg/L; Tramal® 100 mg/mL, Grünenthal GmbH), which was added to drinking water for at least 5 days. Animal well-being was monitored twice daily for the first 5 postoperative days, then assessed daily for up to 7 days and twice weekly thereafter by blinded animal caretakers (AF, RM, LF, PF, and PE) and veterinarians (SZ, DA, HM, and LG). Animals were monitored for their general and eating behavior and the load they placed on the operated-on leg. External appearance and wound status were also monitored. The weight was checked 3 and 7 days after surgery and weekly thereafter. Animals were euthanized at the defined endpoints through cervical dislocation after administering sevoflurane anesthesia to the animals.

Animal Welfare

In total, 24 of the 25 mice included in this study survived to the scheduled endpoint without reaching the predefined abruption criteria. One animal was euthanized because of an iatrogenic femur fracture intraoperatively and was immediately replaced. In the 4-day group, one animal (inoculated with Hi-SA5458) had a distal femur fracture diagnosed with postmortem radiographs. Three animals in the 14-day group (all infected with Hi-SA5458) experienced continuing lameness. To prevent these animals from suffering, analgesics (paracetamol and tramadol) were prolonged in animals infected with Hi-SA5458. On the postmortem radiographs, one animal infected with Hi-SA5458 in the 14-day group exhibited a proximal femur fracture. Both animals experiencing an additional femur fracture were excluded from the clinical scoring analysis at all timepoints. Because these animals received full surgical treatment and the 14-day course of infection was fulfilled, their bacteriological and histopathologic results were included.

Immune Response and Inflammatory Reaction

Preoperative blood samples were taken from the tail vein after putting the animals under anesthesia. Blood samples were also taken on the day of euthanasia (Days 4 or 14) after induction of anesthesia by retro-orbital bleeding. Blood samples were taken in serum tubes and briefly

stored at 4°C, before centrifugation at 2500 rpm for 5 minutes.

The supernatant serum was transferred into 1.5-mL Eppendorf tubes and stored at -20°C until use. Interferon-γ, interleukin-1β, IL-2, IL-4, IL-5, IL-6, IL-10, IL-12p70, keratinocyte chemo attractant/human growth-related oncogene, and tumor necrosis factor-α were then measured using a V-PLEX Proinflammatory Panel 1 (mouse) Kit (Meso Scale Discovery) according to the manufacturer's protocol. As recommended by the manufacturer, samples were incubated overnight at 4°C on the plate to achieve higher detection sensitivity.

Posteuthanasia and Sample Processing

All samples for bacteriologic examination were harvested, with careful attention to the aseptic technique. After the skin and fur were sprayed with 70% ethanol, fur and skin were carefully dissected, and the operated-on left hind leg was separated from the hip. A wedge-shaped piece of soft tissue adjacent to the plate was dissected from the lateral side of the femur for quantitative bacteriology. The remaining soft tissue was once again sutured (6-0 Prolene, Ethicon) to keep the soft tissue in place and avoid possible shrinking artifacts during the fixation process for histologic analysis. Samples of the spleen, kidney, and liver were collected for bacteriologic analyses.

Quantitative Bacteriology

The dissected organs and soft tissue samples were placed in sterile vials containing 4 mL of phosphate-buffered saline. All tissue samples were weighed and subsequently subjected to homogenization (Omni Tissue Homogenizer and Hard Tissue Homogenizing tips, Omni International). To quantify bacteria in the homogenized suspensions, six serial 10-fold dilutions were made from the original suspensions, and triplicate aliquots of all dilutions, as well as the undiluted sample, were placed on blood agar (Oxoid AG). All plates were incubated at 37°C for 24 hours. Bacterial colonies were counted by a blinded investigator (SB) at the dilution yielding the densest yet countable colonies, and the resulting numbers are presented as CFUs per gram of tissue. Furthermore, agar plates were checked again for any signs of slow-growing contaminants after an additional 24 hours at room temperature. To confirm the presence of S. aureus, a latex agglutination assay (Staphaurex, Thermo Scientific) was performed for at least one isolate per mouse.

Histology

Immediately after harvesting the biopsies for bacteriology, we placed the infected legs containing the titanium plate and surrounding soft tissue in 70% methanol. Contact radiographs were taken using a cabinet X-ray system (Model No. 43855A, Faxitron X-Ray Corp) and high-resolution technical films (D4 Structurix DW ETE, Agfa). After fixation, samples were subjected to a dehydration process through ascending concentrations of ethanol and transferred to xylene before being embedded in methyl methacrylate (Sigma-Aldrich). Once cured, two approximately 200-μm-thick longitudinal sections were made through the plate and femur using a Leica 1600 rotating saw microtome (Leica microsystems). These sections were fixed with cyanoacrylate onto Plexiglas slides and ground to a thickness of approximately 100 μm using a microgrinding system. One section per animal was stained with Giemsa eosin.

Histopathologic Evaluation

Histopathologic analysis included the bone and bone marrow, plate interface, and surrounding soft tissue. One veterinary pathologist (DN) with special focus on bone healing and localization of inflammatory changes analyzed Giemsa eosin-stained and methyl methacrylate–embedded specimens. Scoring was performed in a blinded manner, and group allocation was revealed after scoring. Inflammatory changes were rated for polymorphonuclear cell infiltration, necrotizing inflammation, or mononuclear cell infiltration. Semiquantitative assessment of Giemsa-positive stained bacteria was conducted separately for the soft tissue above the plate, soft tissue below the plate, fracture gap, and bone marrow. Bone healing was assessed at the fracture gap and around the implant and screws. Here, osteolysis and osteonecrosis, as well as callus formation at the osteotomy gap, were investigated. According to their severity, changes were semiquantitively graded as follows: absent (0), minimal (1), slight (2), moderate (3), marked (4), and massive (5).

To differentiate between acute and chronic signs of osteomyelitis, the sections were additionally evaluated according to the Histopathological Osteomyelitis Evaluation Score [25]. This score characterizes three features of acute osteomyelitis (A) and two features of chronic osteomyelitis (C). Acute osteomyelitis was assumed by the presence of the following criteria: osteonecrosis (A1), soft tissue necrosis (A2), and neutrophilic granulocyte infiltration (A3). The features indicating chronic osteomyelitis consisted of bone neogenesis or fibrosis (C1) and lymphocyte, macrophage, and plasma cell infiltration (C2). The above criteria for acute (A1 to A3) and chronic (C1 and C2) osteomyelitis were scored from 0 to 5 with respect to their presence in tissue.

Ethical Approval

All animal experiments performed in this study were approved by the ethical committee of the canton of Graubünden, Switzerland (approval number 23/2020), and were conducted in an Association for Assessment and Accreditation for Laboratory Animal Care international accredited facility.

Statistical Evaluation

Descriptive and statistical data analysis was performed and visualized using GraphPad Prism 8 (GraphPad Software). Numeric values are expressed as the mean ± SD or, for values with non-normal distribution, as median values with range. Means were compared using a t-test or two-way analysis of variance across multiple groups. Normal distribution was checked using the Shapiro-Wilk test, and equality of variances was measured using the Levene test. We compared non-normally distributed data using the Mann-Whitney U test. If required, we used the chi-square test and Fisher exact test for comparing categorical variables. Proportions are expressed as percentages with ORs and 95% CI. We used one-way analysis of variance and the Tukey post hoc test to compare cytokine and chemokine levels in serum between the two groups per timepoint. Weight was compared using two-way analysis of variance with repeated measures. For all tests, a p value < 0.05 was considered statistically significant.

Results

Clinical Observations of Change in Body Weight

At 4 days, there was no difference in weight loss between the Hi-SA5458-infected animals and Lo-SA5464-infected animals (mean -0.6 ± 0.1 grams versus -0.8 ± 0.2 grams, mean difference -0.2 grams [95% CI -0.8 to 0.5 grams]; p = 0.43) (Fig. 2A). At 14 days, the Hi-SA5458-infected group lost more weight than did the Lo-SA5464-infected group (mean -1.55 ± 0.2 grams versus -0.8 ± 0.3 grams; mean difference 0.7 grams [95% CI 0.2 to 1.3 grams]; p = 0.02) (Fig. 2B).

Quantitative Bacteriology

On Day 4, the bacterial burden in soft tissue was higher in the Hi-SA5458-infected group (median 6.8 x 10^7 CFU/g, range 2.2 x 10^7 to 2.1 x 10^9 CFU/g) than in the Lo-SA5464 group (median 6.0 x 10^6 CFU/g, range 1.8 x 10^5 to 1.3 x 10^8 CFU/g; difference of medians 6.2 x 10^7; p = 0.03)
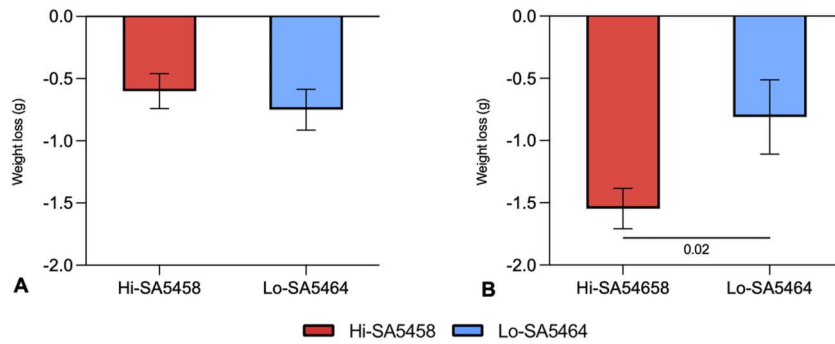
Fig. 2 This figure shows the weight loss in grams of Hi-SA5458- and Lo-SA5464-infected animals at (**A**) 4 days and (**B**) 14 days postoperatively. Data are presented as mean ± SD (five to six animals per group). A color image accompanies the online version of this article.
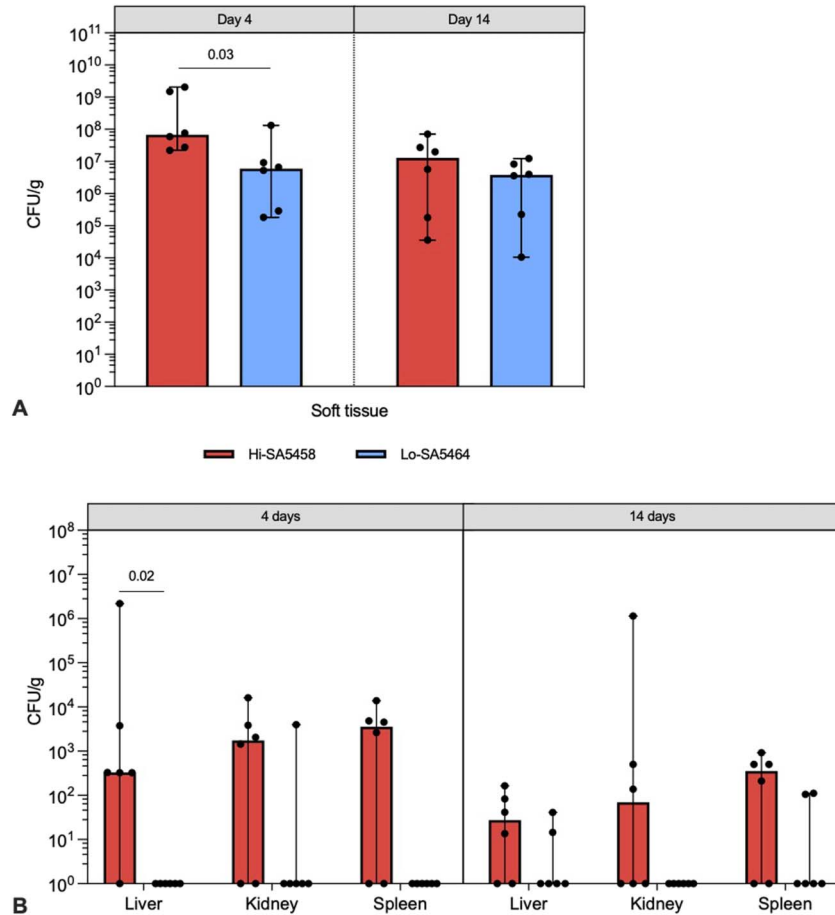

Fig. 3 This figure shows the results of quantitative bacteriology of Hi-SA5458- and Lo-SA5464-infected animals in (**A**) soft tissue samples and (**B**) organ samples (liver, kidney, and spleen) at euthanasia on Days 4 and 14 postoperatively. Results are presented as median with range (six per group). A color image accompanies the online version of this article.

(Fig. 3A). On Day 14, no difference in CFU counts was observed between Hi-SA5458-infected and Lo-SA5464-infected animals (Fig. 3A). Systemic dissemination of bacteria in the liver on Day 4 was greater for mice inoculated with Hi-SA5458 (median 3.3 x 10^2 CFU/g, range 0 to 2.2 x 10^6 CFU/g) than for those with Lo-SA5464 (median 0 CFU/g, range 0 to 0 CFU/g; difference of medians 3.3 x 10^2; p = 0.02) (Fig. 3B). On Day 14, there was no difference in bacterial load (CFU/g) in the organs of animals infected with Hi-SA5458 compared with those infected with Lo-SA5464 (Fig. 3B). Considering both timepoints, the overall proportion of bacteria-positive organ samples was greater in the Hi-SA5458-infected cohort (67% [24 of 36 organs]) than in animals infected with the Lo-SA5464 strain (14% [five of 36 organs]; OR 12.0 [95% CI 3.7 to 36]; p < 0.001).

The bacterial inocula administered to each animal were confirmed within the target range of 5.0 x 10^3 to 2.0 x 10^4 CFU per animal by quantitative bacteriologic analysis. No differences were noted between the mean CFU counts of inocula containing Hi-SA5458 and Lo-SA5464 (mean 1.5 x 10^4 CFU/animal $\pm$ 3.3 x 10^3 versus 1.3 x 10^4 CFU/animal $\pm$ 3.3 x 10^3; mean difference 2.2 x 10^3 CFU/animal [95% CI -2.1 x 10^3 to 6.4 x 10^3 CFU/animal]; p = 0.28).

Through a postmortem bacteriologic evaluation of soft tissue, all mice were confirmed to be infected. In four animals (three liver and one kidney sample), bacteria other than *S. aureus* (based on colony morphology) were identified at the time of euthanasia. In these cases, CFU counts were low and exhibited a variety of colony types, suggesting contamination from the overlying skin, fur, or intestines during processing, and therefore was not considered as an invasive infection.

Immune Response and Inflammatory Reaction

The early stage of infection (Day 4) was characterized by elevated levels of innate immune response cytokines, although no differences were observed between groups (Fig. 4A to 4F). On Day 14, the proinflammatory immune response was more pronounced in Hi-SA5458-inoculated animals than in Lo-SA5464-inoculated animals, as revealed by higher levels of proinflammatory markers observed for interleukin-1β (mean 9.0 $\pm$ 2.2 pg/mL versus 5.3 $\pm$ 1.5 pg/mL; mean difference 3.6 pg/mL [95% CI 2.0 to 5.2 pg/mL]; p < 0.001) (Fig. 4A), IL-6 (mean 458.6 $\pm$ 370.7 pg/mL versus 201.0 $\pm$89.6 pg/mL; mean difference 257.6 pg/mL [95% CI 68.7 to 446.5 pg/mL]; p = 0.006) (Fig. 4B), IL-10 (mean 15.9 $\pm$ 3.5 pg/mL versus 9.9 $\pm$ 1.0 pg/mL; mean difference 6.0 pg/mL [95% CI 3.2 to 8.7 pg/mL]; p < 0.001) (Fig. 4C), and interferon-γ (mean 2.7 $\pm$ 1.9 pg/mL versus 0.8 $\pm$ 0.3 pg/mL; mean difference 1.8

pg/mL [95% CI 0.5 to 3.1 pg/mL]; p =0.002) (Fig 4D). No differences were observed in keratinocyte chemoattractant or human growth-related oncogene (Fig. 4E) and tumor necrosis factor-α (Fig.4F) between Hi-SA5458- and Lo-SA5464-inoculated animals.

Radiographic and Histopathologic Evaluation

Radiographic Signs of Bone Healing

On Postoperative Day 4, qualitative assessment of radiographs in both groups did not show any signs of bone healing or infection-related changes (Fig. 5A and 5B). After 14 days, no callus formation was seen in animals infected with Hi-SA5458. Instead, postmortem radiographs in Hi-SA5458-infected animals showed erodent fracture ends and radiolucent areas adjacent to the screws and plate, suggesting osteolysis (Fig. 5C). Early signs of callus formation at the fracture site were visible in the Lo-SA5464-infected cohort (Fig. 5D).

Histopathologic Signs of Bone Healing

By Day 4, no soft callus or woven bone formation was present in either group (Fig. 6A to 6F). Hi-SA5458-infected animals exhibited visible osteonecrosis (Fig. 6E). By Day 14 (Fig. 7A to 7F), animals inoculated with Hi-SA5458 exhibited osteonecrosis at the fracture gap and bone tissue adjacent to the screws (Fig. 7E). In the Hi-SA5458 cohort, mainly fibrinous tissue was present at the fracture gap (Fig. 7E), while bony callus formation (Fig. 7F) was present in animals inoculated with Lo-SA5464 (mean grade 0.2 $\pm$ 0.4 versus 1.8 $\pm$ 1.2; mean difference -1.6 [95% CI -2.8 to -0.5]; p = 0.008).

Histopathology of Bacterial Microcolonies

Bacterial microcolonies were visible in the soft tissue above (Fig. 8A) and below the plate (Fig. 8B), at the fracture gap (Fig. 8C), and in the bone marrow (Fig. 8D). After 4 days, bacterial microcolonies in Hi-SA5458-infected animals were found to a higher extent below the plate than in Lo-SA5464-infected animals (mean grade 2.7 $\pm$ 0.5 versus 1.3 $\pm$ 1.3; mean difference 1.3 [95% CI 0.1 to 2.5]; p =0.03), at the fracture site (mean grade 1.7 $\pm$ 0.3 versus 0.5 $\pm$ 1.3; mean difference 1.3 [95% CI 0.1 to 2.5]; p =0.03), and in the bone marrow (mean grade 1.7 $\pm$ 1.4 versus 0.2 $\pm$ 0.4; mean difference 1.5 [95% CI 0.3 to 2.7]; p = 0.02) (Fig. 9).

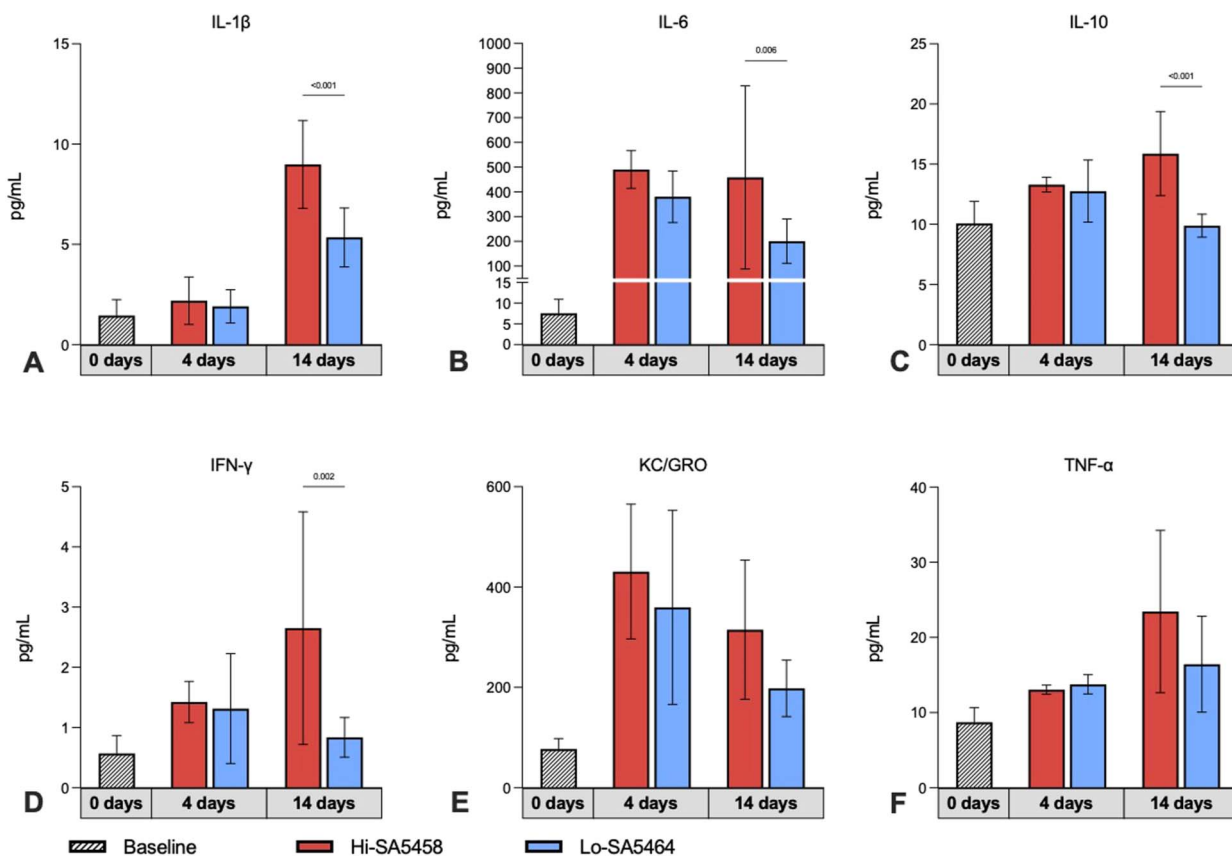By Day 14, the bacterial content below the plate was increased in Hi-SA5458-infected animals compared with

Fig. 4 This figure shows the systemic cytokine profiles for (**A**) interleukin-1β, (**B**) IL-6, (**C**) IL-10, (**D**) interferon-γ, (**E**) keratinocyte chemoattractant/human growth-related oncogene, and (**F**) tumor necrosis factor in serum samples of Hi-SA5456- and Lo-SA5464-infected animals before surgical intervention (Day 0) and at Days 4 and 14 after surgery (six per group). Results of preoperative serum samples of all animals (22) were pooled across timepoints (striped bar). Results are expressed as means ± SDs. One preoperative specimen was excluded because of severe hemolysis and one was excluded because of low specimen volume. A color image accompanies the online version of this article.

their Lo-SA5464-infected counterparts (mean grade 3.3 ± 0.5 versus 2.0 ± 0.6; mean difference 1.3 [95% CI 0.2 to 2.6]; p = 0.02) (Fig. 9). In the bone marrow of the Hi-SA5458-infected cohort, bacteria were detected in similar amounts (mean grade 3.3 ± 0.5) as in Lo-SA5464-infected animals (mean grade 2.6 ± 0.8; mean difference 0.7 [95% CI -0.4 to 1.8]; p = 0.26)

Histopathology of Immune Cells

On Day 4, inflammation with mainly polymorphonuclear cell infiltration was present in both groups, although somewhat more prominent in Hi-SA5458-infected animals (mean grade 2.5 ± 1.0) than in Lo-SA5464-infected animals (mean grade 1.8 ± 1.4; mean difference 0.7 [95% CI 0.001 to 1.4]; p = 0.0498) (Fig. 10A). In the bone marrow, inflammation consisting of polymorphonuclear cell infiltration (mean grade 3.3 ± 0.5 versus 2.0 ± 0.6; mean difference 1.3 [95% CI 0.2 to 2.6]; p < 0.001) and necrotic

changes (mean grade 3.0 ± 0 versus 1.8 ± 1.2; mean difference 1.2 [95% CI 0.2 to 2.1]; p = 0.016) was increased in the Hi-SA5458-inoculated group compared with their Lo-SA5464-inoculated counterparts. After 14 days, necrotizing inflammation was still in progress in Hi-SA5458-infected animals and more pronounced than in the Lo-SA5464-infected cohort (mean grade 2.5 ± 1.5 versus 1.7 ± 1.4; mean difference 0.8 [95% CI 0.2 to 1.4]; p = 0.007) (Fig. 10A). The histologic inflammatory reaction shifted toward mixed inflammation with immigration of mononuclear cells in both cohorts up to Day 14 compared with Day 4 (Fig. 10A).

Histopathologic Osteomyelitis Evaluation Score

On Day 4, acute patterns of osteomyelitis (osteonecrosis, granulocyte infiltration, and soft tissue necrosis) were present in both groups (Fig. 10B). Animals inoculated with Hi-SA5458 exhibited higher severity scores for granulocyte
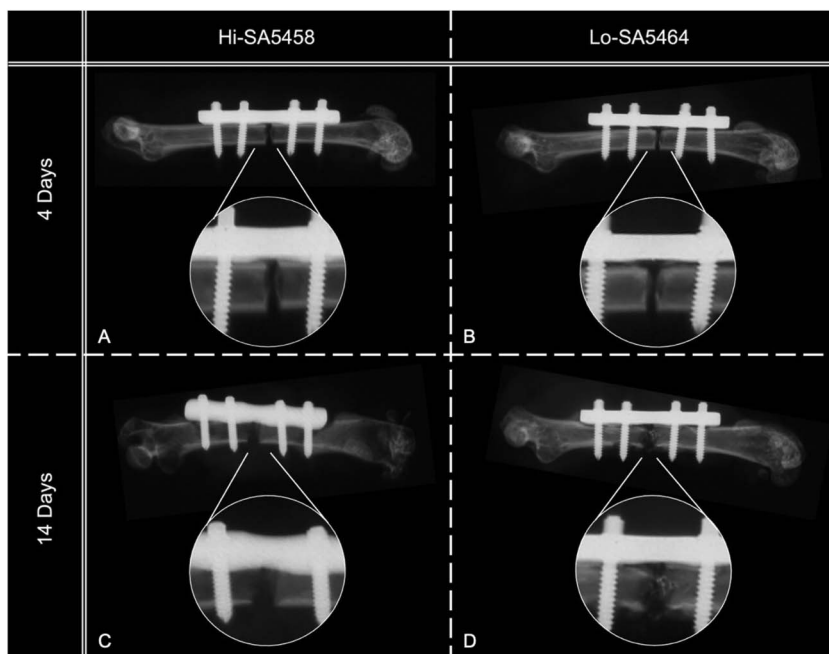
Fig. 5 This figure shows representative postmortem contact radiographs of Hi-SA5456- and Lo-SA5464-inoculated animals with a single osteotomy stabilized with a four-hole MouseFix locking plate (**A and B**) 4 days and (**C and D**) 14 days postoperatively. On Day 4, no signs of bone healing were observed in (**A**) Hi-SA5456- or (**B**) Lo-SA5464-infected animals. Hi-SA5458-infected mice displayed osteolytic lesions adjacent to the plate and screws and at the fracture site (**C**), whereas Lo-SA5464-infected mice showed signs of the beginning of bone healing and callus formation (**D**) at Day 14 postoperatively.

infiltration at Day 4 than Lo-SA5464-infected animals (mean severity score 2.5 ± 0.3 versus 1.8 ± 0.3; mean difference 0.7 [95% CI 0.1 to 1.4]; p = 0.03) (Fig. 10B). By Day 14 postoperatively, both groups had chronic signs of osteomyelitis consisting of infiltration with mononuclear cells (Fig. 10B). Bone neogenesis was more pronounced in Lo-SA5464-infected animals than in Hi-SA5458-infected animals (mean severity score 1.5 ± 0.4 versus 2.3 ± 0.5; mean difference -0.8 [95% CI -1.5 to -0.2]; p = 0.01), while Hi-SA5458-inoculated animals exhibited a higher degree of osteonecrosis (mean severity score 3.0 ± 0.4 versus 2.2 ± 0.7; mean difference 0.8 [95% CI 0.2 to 1.5]; p = 0.01). However, granulocytic inflammation in the soft tissue, bone, and bone marrow were still present on Day 14, indicating persistent acute infection in both groups.

Discussion

Recently, there has been a growing understanding of the pathogenesis and virulence of *S. aureus* in a variety of diseases such as pneumonia, sepsis, skin and soft tissue infections, and surgical site infections [6]. A limited number of osteomyelitis models, most of which compared knockout strains with respect to individual virulence factors and used laboratory strains, have already provided valuable insights into the context of bone infections [3, 6, 29]. In prior in vitro and in vivo studies, clinical *S. aureus* strains isolated from acute and chronic cases differed in cytotoxicity, mortality, virulence, and host immune response, and were associated with increased intra-osteoblastic persistence and biofilm formation [14]. However, the clinical relevance of the causative pathogen and its virulence characteristics in fracture-related infections remains to be determined, especially in clinical isolates [3, 6, 14]. The present study was designed to investigate whether two different clinical courses of infection and the results of the previously performed virulence testing of two clinical strains (Hi-SA5458 and Lo-SA5464) are reflected in a murine model of fracture-related infection. Compared with Lo-SA5464-infected animals, infection with Hi-SA5458 was observed to be more severe according to some key outcome parameters, such as increased bacterial load in quantitative bacteriology (local tissues and organs) and semiquantitative histopathologic grading. Furthermore, infection with Hi-SA5458 was
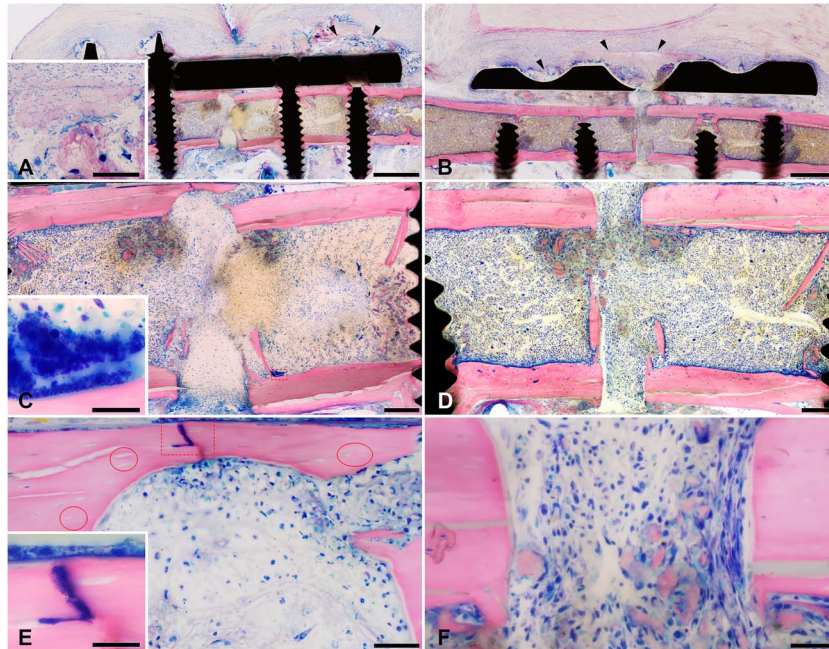
Fig. 6 This figure shows representative microscopic images of Giemsa eosin-stained methyl methacrylate–embedded mouse femoral sections of Hi-SA5458-infected animals and Lo-SA5464-infected animals 4 days postoperatively (bone is stained pink, connective and soft tissue are stained rose, and cell nuclei are dark blue; the fracture site is either complete or only its cis or trans part is shown). Marked tissue necrosis was visible in (**A**, black arrow heads) Hi-SA5458-infected and (**B**, black arrow heads) Lo-SA5464-infected animals. Giemsa-positive coccoid bacteria were visible in (**C**, red square, inset) Hi-SA5458-infected animals. The straight cutting lines show the absence of new bone formation at the bone stumps in (**C**) Hi-SA5458-infected and (**D**) Lo-SA5464-infected animals. In (**E**) Hi-SA5458-infected animals (red circles), empty lacunae indicating osteonecrosis, the presence of a mainly polymorphonuclear or granulocytic inflammation accompanied by (**E**, red square, inset) Giemsa-positive coccoid bacteria were observed. Osteonecrosis was less pronounced in (**F**) animals infected with Lo-SA5464 and the inflammation was more mononuclear (no Giemsa-positive coccoid bacteria in this field of view). Artefacts: (**D**) There was black debris from the Gigli saw used to create the osteotomy at the initial surgery. (**A, B**) Cyan blue–stained, round structures in the soft tissue were monofilament sutures placed postmortem to fix the soft tissue to avoid shrinkage artefacts. Images were taken at 2 x (A and B: scale bar 1 mm), 7.5 x (C and D: scale bar 200 mm), 40 x (E and F: scale bar 50 mm), and 100 x oil (insets: scale bar 20 mm). A color image accompanies the online version of this article.

characterized by more-pronounced systemic dissemination, indicating high rates of bacteremia. Regarding bone remodeling processes, increased osteolysis and osteonecrosis were observed in animals infected with Hi-SA5458, whereas bone healing was evident at Day 14 in animals infected with Lo-SA5464. For a translational use of these findings, the virulence profiles of *S. aureus* could guide our treatment decisions in the future in a case- and pathogen-specific manner. Thus, one approach to fracture-related infections with high-virulence strains might be the development of antivirulence compounds, particularly to treat or prevent septic dissemination.

Limitations

This study was based on a comparative examination of only two isolates derived from two individual patients, and therefore no reliable conclusion can be drawn regarding an overall relationship between specific virulence properties and the clinical presentation of fracture-related infection. Additionally, the study design does not allow for a definitive link between the exact mechanisms or factors and observed differences in the severity of infection because multiple mutations were described in the genome of both strains studied here [14]. However, as a proof-of-principle study, it is
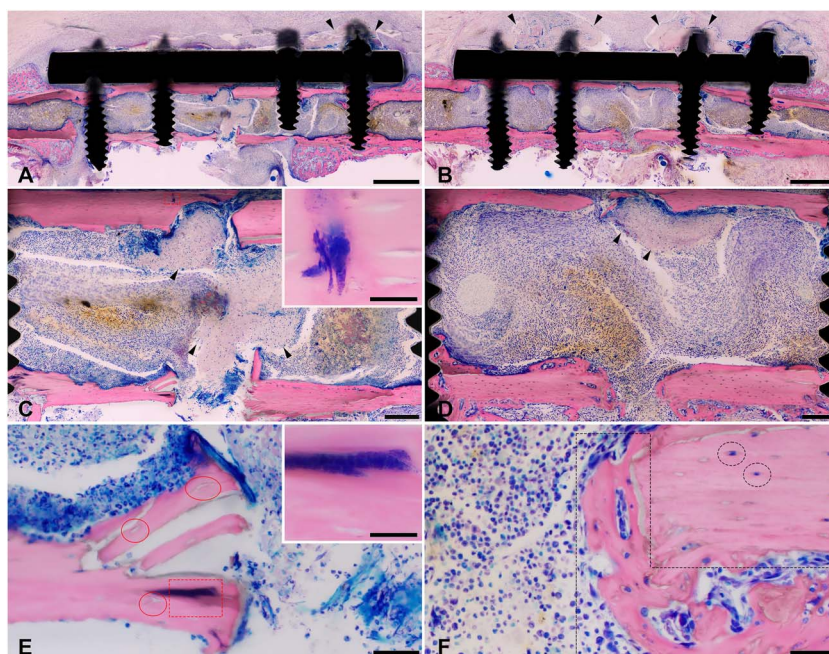
Fig. 7 This figure shows representative microscopic images of Giemsa eosin-stained methyl methacrylate–embedded mouse femoral sections of Hi-SA5458-infected animals and Lo-SA5464-infected animals 14 days postoperatively (bone is stained pink, connective and soft tissue are rose, and cell nuclei are dark blue; the fracture site is either complete or only its trans part is shown). Marked tissue necrosis above the plate was visible in (**A**, black arrowheads) Hi-SA5458-infected animals and (**B**, black arrowheads) Lo-SA5464-infected animals. In Hi-SA5458 (**C**, black arrowheads), necrosis inside the bone marrow was present. Giemsa-positive coccoid bacteria were visible in (**C**, red square, see inset) Hi-SA5458-infected animals and less present in (**D**) Lo-SA5464-infected animals. (**E**) In animals infected with Hi-SA5458, mainly polymorphonuclear cell infiltration was observed, accompanied by (**E**, red square, inset) Giemsa-positive coccoid bacteria. In (**E**) Hi-SA5458-infected animals, the straight cutting lines on the bone stumps indicate no new bone formation, while (**E**, red circles) the presence of empty lacunae indicates osteonecrosis. In contrast, osteonecrosis in (**F**) Lo-SA5464-infected animals was less pronounced (**F**, black circles; lacunae are occupied by osteocytes), and the cutting lines were not completely straight but (**F**, black dashed polygon) limited new bone formation was recorded. Additionally, inflammation in (**F**) Lo-SA5464-infected animals was characterized by mixed infiltration mainly with mononuclear cells (no Giemsa-positive coccoid bacteria were found in this field of view). Artefacts: Cyan blue–stained, round structures in the soft tissue (**A, B**) were monofilament sutures placed postmortem to fix the soft tissue to avoid shrinkage artefacts. Images were taken at 2 x (A and B: scale bar 1 mm), 7.5 x (C and D: scale bar 200 mm), 40 x (E and F: scale bar 50 mm), and 100 x oil (insets: scale bar 20 mm). A color image accompanies the online version of this article.

encouraging that mutations in virulence factors may lead to different clinical courses that may remain stable even when transferred to a different host. Two animals infected with Hi-SA5458 experienced implant loosening and an additional femur fracture that was expected to substantially influence the clinical evaluation, and therefore these animals were excluded from these analyses. Because these animals were included in the bacteriologic and histologic analysis, there may have been more severe bone and soft tissue destruction and increased local and systemic inflammation [8]. Conversely, bone resorption, implant loosening, and ultimately implant failure could have been because of a more-aggressive infection, leading to additional fractures of the affected bone [8]. Because this could not be conclusively clarified, we refrained from excluding and replacing these animals to avoid unnecessary harm to further animals. Finally, no chronic infection could be established by Day 14, as evidenced by persistent granulocytic infiltration. Although osteoneogenesis
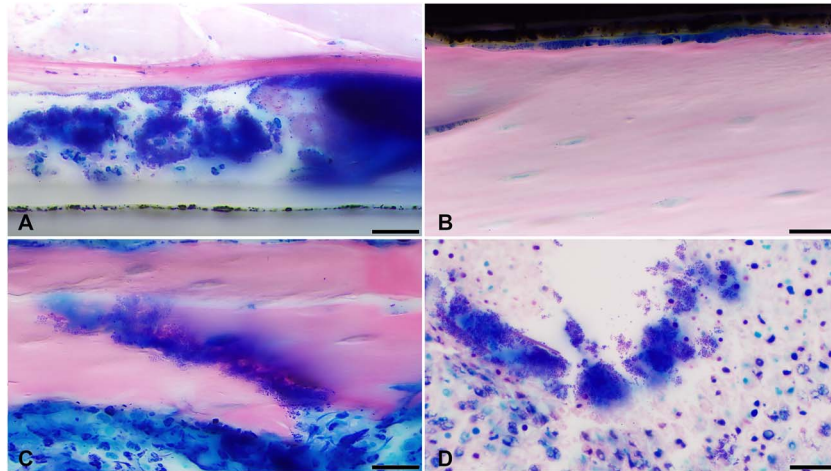
Fig. 8 Representative images of Giemsa eosin-stained and methyl methacrylate–embedded sections are shown, displaying microscopically detected bacterial microcolonies (**A**) in the soft tissue above and (**B**) below the plate, (**C**) at the fracture gap, and (**D**) in the bone marrow. Images were taken at 100 x (scale bar 20 mm).

as a chronic osteomyelitis sign was increased in the Lo-SA5464-infected cohort, a longer observation period might have revealed more distinct differences. However, a longer observation period would likely have resulted in high exclusion rates for animal welfare reasons, because animals infected with Hi-SA5458 already required additional pain medication throughout the 14-day period to prevent them from suffering. Additionally, because we focused on the

histomorphologic pathogenesis of bone infection, no quantitative bacteriology of bone was performed. However, semi-quantitative histologic grading of bacterial microcolonies suggests the bacterial load in bone may have been elevated, which has also been observed in soft tissue samples from Hi-SA5458-infected animals. Finally, these histomorphologic analyses can always be subjective to some degree, even if the pathologist is experienced. To keep these analyses as
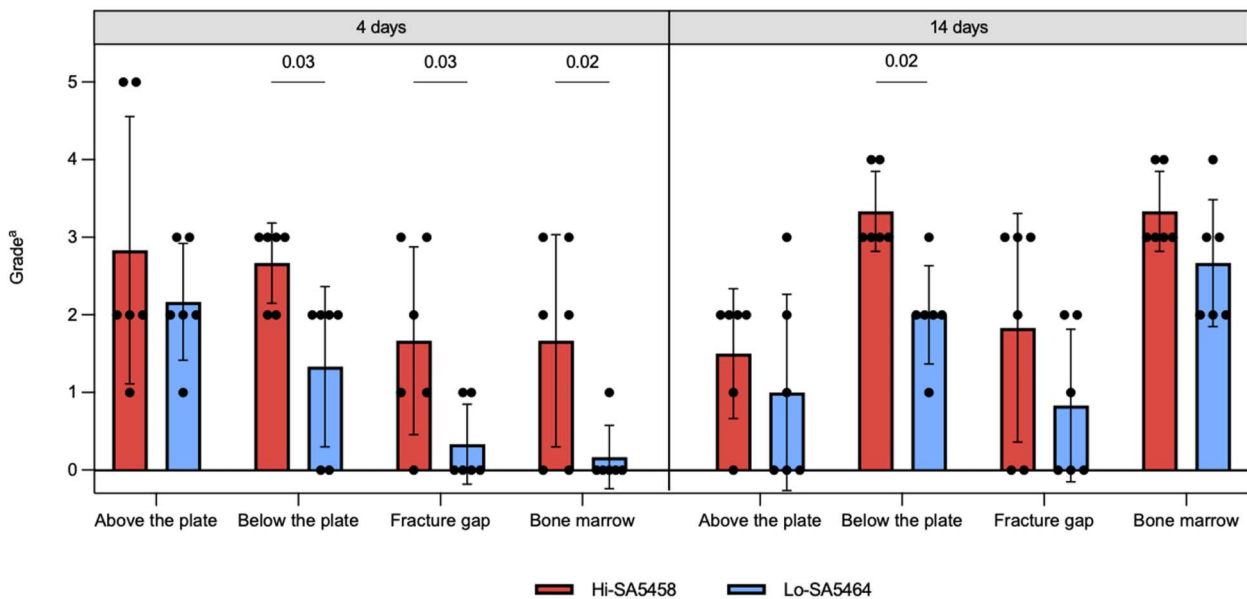

Fig. 9 This figure shows the histopathologic semiquantitative grading of bacterial microcolonies in each group (means ± SDs; six per group). [a]Grade 0 = absent; 1 = minimal; 2 = slight; 3 = moderate; 4 = marked; 5 = massive or complete.
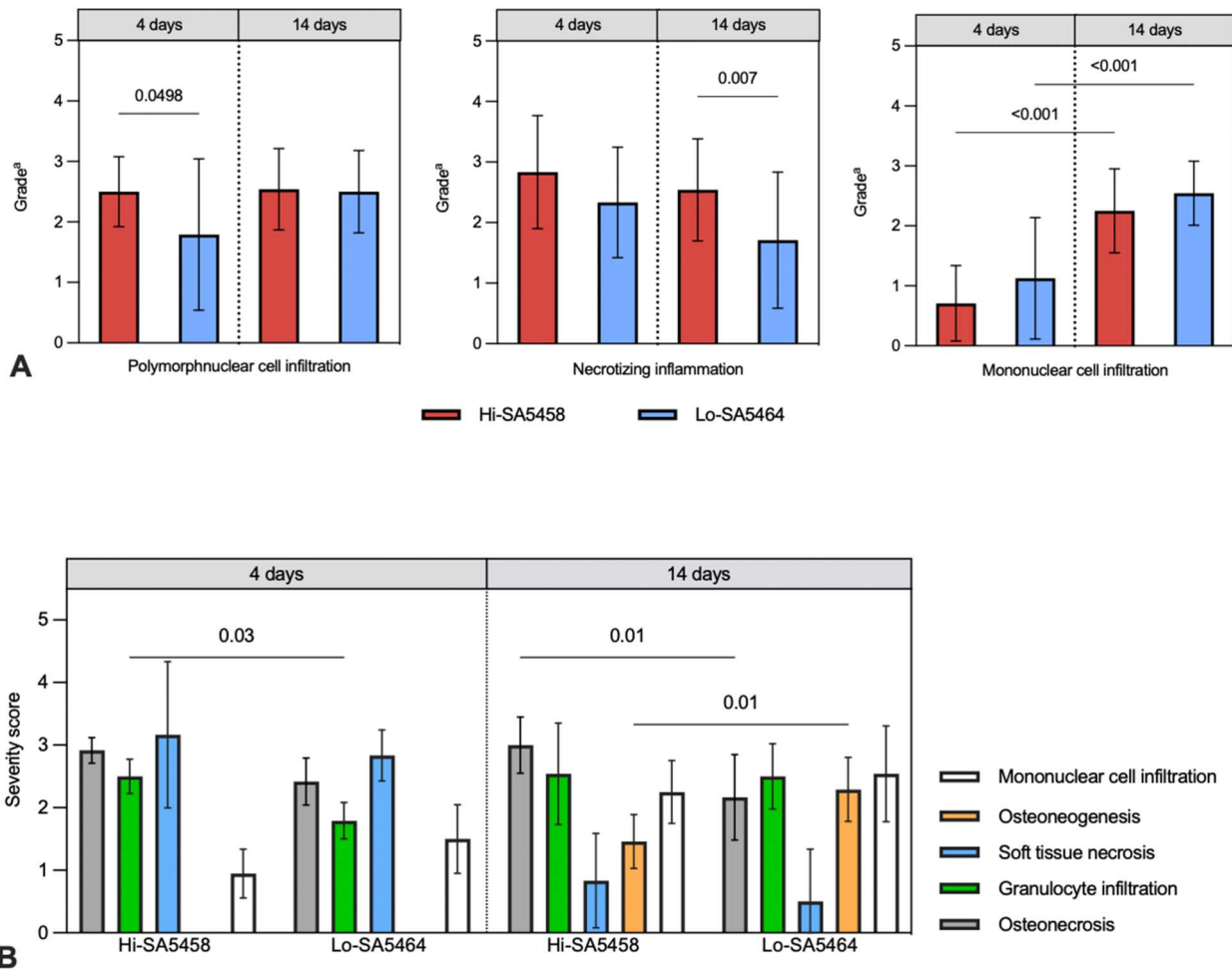
Fig. 10 This figure shows the (**A**) histopathologic semiquantitative grading of local inflammatory reactions, consisting of polymorphonuclear cell infiltration, necrotizing inflammation, and mononuclear cell infiltration. Values are presented as means ± SDs (six per group). ᵃGrade 0 = absent; 1 = minimal; 2 = slight; 3 = moderate; 4 = marked; 5 = massive or complete. (**B**) This image shows the histopathologic osteomyelitis evaluation severity scores of animals infected with Hi-SA5458 or Lo-SA5464 assessed at 4 and 14 days postoperatively. Acute features from left to right were osteonecrosis (gray), granulocyte infiltration (green), and soft tissue necrosis (blue). Chronic signs consisted of osteoneogenesis or fibrosis (orange) and mononuclear cell infiltration (white). The severity score is presented as means ± SDs (six per group).

objective as possible, the pathologist was blinded to group assignment.

Discussion of Key Findings

Differences in the Pathophysiology and Severity of Infection

The bacterial burden was lower in animals infected with Lo-SA5464, while the Hi-SA5458-infected cohort exhibited a more-pronounced systemic dissemination of infection. These findings shared parallels with the infection of the patient who experienced a septic course of acute fracture-related infection, in which Hi-SA5458 infection was associated with high C-reactive protein levels, increased pain, and fever [14]. In

orthopaedics, detailed data regarding the number of patients who experience a septic course with *S. aureus* bacteremia after fracture-related infection are lacking; however, sepsis is one of the most feared complications [1, 7, 20]. Recent research has focused on developing antivirulence compounds to combat *S. aureus* infections [6, 10]. For high-virulence strains, such as the one studied here, targeting the virulence factors of the pathogen may be a promising approach to reduce the severity of infection, especially in septic courses. This approach could be particularly useful in cases where traditional antibiotics are not effective because of antibiotic resistance or toxicity [5]. Conversely, reduced pathogenicity and toxicity may result in slower progression of infection but provide better survival and persistence in the host, which may require prolonged antibiotic treatment or a more radical surgical approach because of

increased biofilm formation and sessile pathogens in a quasi-dormant state [3, 21, 29]. Trouillet-Assant et al. [27] yielded results similar to those presented here. They demonstrated that isolates from recurrent and chronic bone and joint infections were less virulent, as measured by the number of bacteria in the harvested organs and the overall mortality rate, but were stronger producers of mature biofilms. In contrast to the existence of genomic differences between the strains studied here, the authors did not observe genomic-level changes in those recurrent isolates and concluded that conversion to chronic *S. aureus* bone and joint infection is more likely associated with in vivo phenotypic adaptation of the bacterium [27]. The reasons for more systemic spread of infection in all animals infected with Hi-SA5458 may be due to its ability to survive and replicate intracellularly, as shown in osteoblast-like cells [14]. Findings derived from sepsis models suggest that intracellular survival and proliferation in neutrophils are key to the transmission of infection from primary to secondary sites. Via the bloodstream, *S. aureus* reaches the liver, where it can form microlesions. Subsequently, it is presumably released into the bloodstream, penetrates neutrophils, and is carried to other organs, where further abscesses can develop [5]. Likewise, on Day 4, the liver was primarily affected in animals infected with Hi-SA5458, but bacteria spread to the kidneys and spleen as the infection progressed. Yet, how bacterial virulence contributes to fracture-related infections and their complications has not been fully elucidated, which would be crucial knowledge for the development of new treatment strategies such as antivirulence agents and immunomodulatory approaches. Future studies should focus on characterizing virulence in a broad range of clinical *S. aureus* isolates in relation to human clinical courses. By using a stepwise knockout model of virulence genes in Hi-SA5458 isolates and comparative studies in vitro and in vivo, it would be interesting to determine whether the severity of infection becomes more similar to that induced by Lo-SA5464, providing potential targets for antivirulent or immunomodulatory approaches.

Influence of Genomic Mutations in Virulence Regulatory Systems on the Course of Fracture-related Infection

Infection with Lo-SA5464, which contained mutations in virulence-regulating genes (agrC and sarU), was characterized by less local inflammation, lower bacterial burden, and systemic dissemination, as well as less pronounced osteolysis and osteonecrosis. Further, bone healing was enhanced in animals infected with Lo-SA5464. The Lo-SA5464 strain harbors several mutations, resulting in truncated genes encoding bacterial toxins and virulence regulators, among them mutations of the agrC and the sarU gene, which are intact in Hi-SA5458 [14]. As key mediators, their expression leads to increased production of cytotoxic substances such as phenol-soluble modulins,

hemolysins, leucocidins, and MHC Class II analog protein [2, 11]. These exoproteins are believed to substantially contribute to increased cell death and bone destruction, systemic spread of infection, and maintenance of a proinflammatory environment while evading host immune defenses [3, 11, 19, 29]. Conversely, attenuation of the Agr system in osteomyelitis models decreases infection severity, including the number of abscesses, tissue and bone destruction, and histologic inflammation [2, 4, 21, 27]. Consistent with the results presented here, studies comparing recurrent Agr-deficient strains with initial isolates with intact Agr systems in chronic osteomyelitis also found decreased cytokine release [3, 27]. Interestingly, loss of function in the Agr system is commonly detected in chronic infections [9, 24, 29]. Nevertheless, future studies are needed to determine whether the mechanisms described here are driven at the genomic level or whether they more closely reflect in vivo adaptive strategies expressed at transcriptional and translational levels [3, 27]. Analysis of bacterial genome expression in clinical samples could provide comprehensive insight into the upregulation or downregulation of virulence factors during acute and chronic fracture-related infections.

Parallels of In Vivo Data From Animal Models to Clinical Use in Humans

To the best of our knowledge, this is the first study to investigate whether different clinical courses of fracture-related infections in humans associated with mutations in virulence regulator systems are reflected in a standardized murine fracture-related infection model and nonvertebral animal models. Overall, our findings in animals infected with Hi-SA5458 correlated well with the clinical presentation of the patient, who suffered from acute fracture-related infection accompanied by high C-reactive protein levels, increased pain, and fever because of Hi-SA5458 infection [14]. Conversely, infection with Lo-SA5464 resulted in a less-invasive infection in both the human host and the animals investigated here. In previous work, larvae of *Galleria mellonella* were infected with various clinical *S. aureus* isolates, and survival of larvae was observed for 5 days after infection in terms of differential lethality [16]. The high lethality of Hi-SA5458 infection in the *Galleria mellonella* model is consistent with the increased severity observed in the human host and the more aggressive infection detected in the present mouse model. In accordance with the 3R principles (replacement, reduction, and refinement) for animal welfare introduced by Russell and Burch [23], the *Galleria mellonella* model can serve as an intermediate step between in vitro assays and in vivo vertebrate models to study implant-associated infections, reducing the need for vertebrate models in the future [15].

Conclusion

Similar to septic infection in the human host, we found more-severe systemic and local infection caused by Hi-SA5458 compared with a milder course of infection induced by Lo-SA5464. Thus, there is strong support that the course of infection is not only influenced by host factors or the duration of infection (acute versus chronic), but that pathogenic virulence also plays a crucial role in fracture-related infections. By identifying specific pathogen-related factors that influence the clinical severity of fracture-related infection, this could guide future treatment decisions regarding the extent of surgical treatment and antimicrobial therapy. Following sepsis models, the efficacy of compounds that target virulence factors and thereby attenuate the virulence of *S. aureus* should be investigated in fracture-related infections. If promising, this could introduce a new and additional pharmacologic therapy for bone and joint infections in the long term, which could be particularly important in preventing septic infection. Future studies should focus on characterizing *S. aureus* virulence at the genomic and transcriptomic levels in a broader cohort of clinical isolates and patients and how this relates to the clinical presentation of fracture-related infections in humans. Furthermore, in vitro and in vivo comparisons of knockout versus wildtype strains for specific virulence systems, including the *S. aureus* strains studied here, may reveal whether our observations are reproducible and what genomic characteristics are attributable to increased or attenuated virulence of *S. aureus* in fracture-related infections.

References

1. Bezstarosti H, Van Lieshout EMM, Voskamp LW, et al. Insights into treatment and outcome of fracture-related infection: a systematic literature review. *Arch Orthop Trauma Surg*. 2019;139:61-72.
2. Blevins JS, Elasri MO, Allmendinger SD, et al. Role of *sarA* in the pathogenesis of *Staphylococcus aureus* musculoskeletal infection. *Infect Immun*. 2003;71:516-523.
3. Butrico CE, Cassat JE. Quorum sensing and toxin production in Staphylococcus aureus osteomyelitis: pathogenesis and paradox. *Toxins (Basel)*. 2020;12:516.
4. Cassat JE, Hammer ND, Campbell JP, et al. A secreted bacterial protease tailors the Staphylococcus aureus virulence repertoire to modulate bone remodeling during osteomyelitis. *Cell Host Microbe*. 2013;13:759-772.
5. Cheung GYC, Bae JS, Liu R, Hunt RL, Zheng Y, Otto M. Bacterial virulence plays a crucial role in MRSA sepsis. *PLoS Pathog*. 2021;17:e1009369.
6. Cheung GYC, Bae JS, Otto M. Pathogenicity and virulence of *Staphylococcus aureus*. *Virulence*. 2021;12:547-569.
7. Foster AL, Moriarty TF, Trampuz A, et al. Fracture-related infection: current methods for prevention and treatment. *Expert Rev Anti Infect Ther*. 2020;18:307-321.
8. Foster AL, Moriarty TF, Zalavras C, et al. The influence of biomechanical stability on bone healing and fracture-related infection: the legacy of Stephan Perren. *Injury*. 2021;52:43-52.
9. Fraunholz M, Bernhardt J, Schuldes J, Dabiel R, Hecker M, Sinha B. Complete genome sequence of Staphylococcus aureus 6850, a highly cytotoxic and clinically virulent methicillin-sensitive strain with distant relatedness to prototype strains. *Genome Announc*. 2013;1:e00775-13.
10. Greenberg M, Kuo D, Jankowsky E, et al. Small-molecule AgrA inhibitors F12 and F19 act as antivirulence agents against gram-positive pathogens. *Sci Rep*. 2018;8:14578.
11. Jenul C, Horswill AR. Regulation of Staphylococcus aureus virulence. *Microbiol Spectr*. 2018;6:10.1128.
12. Kuehl R, Tschudin-Sutter S, Morgenstern M, et al. Time-dependent differences in management and microbiology of orthopaedic internal fixation-associated infections: an observational prospective study with 229 patients. *Clin Microbiol Infect*. 2019;25:76-81.
13. Loughran AJ, Gaddy D, Beenken KE, et al. Impact of sarA and phenol-soluble modulins on the pathogenesis of osteomyelitis in diverse clinical isolates of Staphylococcus aureus. *Infect Immun*. 2016;84:2586-2594.
14. Mannala GK, Koettnitz J, Mohamed W, et al. Whole-genome comparison of high and low virulent Staphylococcus aureus isolates inducing implant-associated bone infections. *Int J Med Microbiol*. 2018;308:505-513.
15. Mannala GK, Rupp M, Alagboso F, et al. Galleria mellonella as an alternative in vivo model to study bacterial biofilms on stainless steel and titanium implants. *ALTEX*. 2021;38:245-252.
16. Metsemakers WJ, Kuehl R, Moriarty TF, et al. Infection after fracture fixation: current surgical and microbiological concepts. *Injury*. 2018;49:511-522.
17. Metsemakers WJ, Morgenstern M, McNally MA, et al. Fracture-related infection: a consensus on definition from an international expert group. *Injury*. 2018;49:505-510.
18. Morgenstern M, Kuehl R, Zalavras CG, et al. The influence of duration of infection on outcome of debridement and implant retention in fracture-related infection. *Bone Joint J*. 2021;103:213-221.
19. Muthukrishnan G, Masters EA, Daiss JL, Schwarz EM. Mechanisms of immune evasion and bone tissue colonization that make Staphylococcus aureus the primary pathogen in osteomyelitis. *Curr Osteoporos Rep*. 2019;17:395-404.
20. Petti CA, Sanders LL, Trivette SL, Briggs J, Sexton DJ. Postoperative bacteremia secondary to surgical site infection. *Clin Infect Dis*. 2002;34:305-308.
21. Roper PM, Eichelberger KR, Cox L, et al. Contemporary clinical Isolates of Staphylococcus aureus from pediatric osteomyelitis patients display unique characteristics in a mouse model of hematogenous osteomyelitis. *Infect Immun*. 2021;89:e0018021.
22. Rupp M, Baertl S, Walter N, Hitzenbichler F, Ehrenschwender M, Alt V. Is there a difference in microbiological epidemiology

Wolters Kluwer

and effective empiric antimicrobial therapy comparing fracture-related infection and periprosthetic joint infection? A retrospective comparative study. *Antibiotics (Basel)*. 2021;10:921.

23. Russell WMS, Burch RL. The principles of humane experimental technique. *Med J Aust*. 1960;1:500-500.

24. Suligoy CM, Lattar SM, Noto Llana M, et al. Mutation of Agr is associated with the adaptation of *Staphylococcus aureus* to the host during chronic osteomyelitis. *Front Cell Infect Microbiol*. 2018;8:18.

25. Tiemann A, Hofmann GO, Krukemeyer MG, Krenn V, Langwald S. Histopathological Osteomyelitis Evaluation Score (HOES) – an innovative approach to histopathological diagnostics and scoring of osteomyelitis. *GMS Interdiscip Plast Reconstr Surg DGPW*. 2014;3:Doc08.

26. Torbert JT, Joshi M, Moraff A, et al. Current bacterial speciation and antibiotic resistance in deep infections after operative fixation of fractures. *J Orthop Trauma*. 2015;29:7-17.

27. Trouillet-Assant S, Lelièvre L, Martins-Simões P, et al. Adaptive processes of Staphylococcus aureus isolates during the progression from acute to chronic bone and joint infections in patients. *Cell Microbiol*. 2016;18:1405-1414.

28. Tschudin-Sutter S, Frei R, Dangel M, et al. Validation of a treatment algorithm for orthopaedic implant-related infections with device-retention-results from a prospective observational cohort study. *Clin Microbiol Infect*. 2016;22:457.e1-9.

29. Tuchscherr L, Pöllath C, Siegmund A, et al. Clinical *S. aureus* isolates vary in their virulence to promote adaptation to the host. *Toxins (Basel)*. 2019;11:135.